CI-based QoS-Constrained Transmit Signal Design for DFRC Systems with One-Bit DACs

Zheyu Wu*†, Wei-Kun Chen‡, Ya-Feng Liu*, and Christos Masouros§
*LSEC, ICMSEC, AMSS, Chinese Academy of Sciences, Beijing, China
†School of Mathematical Sciences, University of Chinese Academy of Sciences, Beijing, China
‡School of Mathematics and Statistics, Beijing Institute of Technology, Beijing, China
§Department of Electronic and Electrical Engineering, University College London, London, UK
Email: {wuzy, yafliu}@lsec.cc.ac.cn, chenweikun@bit.edu.cn, c.masouros@ucl.ac.uk

***Abstract*—In this paper, we investigate the transmit signal design problem for a dual-functional radar-communication (DFRC) system equipped with one-bit digital-to-analog converters (DACs). Specifically, the one-bit DFRC waveform is designed to minimize the difference between the transmitted beampattern and a desired one, while ensuring constructive interference (CI)-based QoS constraints for communication users. The formulated problem is a discrete optimization problem with a nonconvex objective function and many linear constraints. To solve it, we first propose a penalty model to transform the discrete problem into a continuous one. Then, we propose an inexact augmented Lagrangian method (ALM) framework to solve the penalty model. In particular, the ALM subproblem at each iteration is solved by a custom-designed block successive upper-bound minimization (BSUM) algorithm, which admits closed-form updates and thus makes the ALM computationally efficient. Simulation results verify the superiority of the proposed approach over the existing ones in both the radar and communication performance.**

***Index Terms*—Augmented Lagrangian method, dual-functional radar communication, one-bit digital-to-analog converters, penalty method.**

I. Introduction

The dual-functional radar-communication (DFRC) system integrates radar and communication functionalities on one platform, attracting significant attention for its capability to save spectrum and hardware resources [1]–[4]. When employed with massive multiple-input multiple-output (MIMO) [5], the DFRC system can further attain enhanced radar and communication performance, as the increased number of antennas offers greater flexibility to mitigate the multiuser interference and shape the spectral beampattern for radar applications. However, a practical issue associated with massive MIMO technology is its high hardware cost and energy consumption. A promising way of addressing this challenge is to employ one-bit digital-to-analog converters (DACs) at each antenna element, which not only minimizes the hardware cost of DACs but also enables the use of the most energy efficient power amplifiers (PAs) [6].

Numerous research efforts have been devoted to one-bit precoding designs and analysis for massive MIMO communication systems [7]–[14]. In particular, nonlinear symbol-level precoding schemes, where the transmit signal is designed based on both the channel and the data symbols, have demonstrated significantly superior performance compared to classical linear precoding schemes [7]. Furthermore, in the context of nonlinear symbol-level precoding, constructive interference (CI) has been shown to be a better performance metric to optimize than traditional mean square error (MSE) [15]. This is because the CI metric exploits the multiuser interference by shaping it to be constructive to the signal of interest, while the MSE metric aims to suppress all the interference.

Despite thorough and extensive studies of one-bit precoding in massive MIMO communication systems, there are very few works studying the design of the one-bit transmit signal for DFRC systems. The only works along this direction are [16]–[18], all of which used the MSE as the communication metric. The CI metric, though widely and successfully adopted in one-bit communication systems [8], [9], [12], has not yet been employed in one-bit DFRC waveform designs (possibly due to its technical difficulty). It is worth mentioning that the works [19]–[21] adopted the CI metric for DFRC waveform design, but they did not consider the one-bit scenario. Furthermore, the existing works on one-bit DFRC waveform design focused on either minimizing the communication MSE under the radar Cramer-Rao bound (CRB) constraint [16] or jointly optimizing the radar beampattern and communication MSE [17], [18]. There is still a lack of exploration in one-bit DFRC transmit signal designs for the practical case where the goal is to optimize the radar performance with *a guaranteed communication QoS requirement*.

In this paper, we study the one-bit transmit signal design problem for the MIMO DFRC system. In sharp contrast to all of the previous works [16]–[18], we employ CI as the communication metric and formulate the problem as the minimization of the difference between the designed beampattern and a desired one, subject to the CI-based QoS requirement constraints of communication users and the one-bit constraints. To solve the formulated problem, we first introduce a penalty model to deal with the discrete one-bit constraint and then propose an inexact augmented Lagrangian method (ALM) framework for solving the penalty model. In particular, at each iteration of the inexact ALM framework, a block successive upper-bound minimization (BSUM) algorithm is custom-designed to solve the ALM subproblem by carefully exploiting the problem structure. Simulation results demonstrate the effectiveness of the proposed approach in both the radar and communication performance.

II. System model and problem formulation

A. System Model

Consider a DFRC system that simultaneously serves K single-antenna users and performs a sensing task. The DFRC system is equipped with N transmit antennas in a uniform linear array (ULA). To achieve hardware-efficiency in the DFRC system, we assume that one-bit DACs are employed. Let $\mathbf{X} = [\mathbf{x}_1, \mathbf{x}_2, \ldots, \mathbf{x}_T] \in \mathbb{C}^{N\times T}$ be the transmit signal matrix, where $\mathbf{x}_t$ is the transmit signal vector in the t-th time slot. Due to one-bit DACs, each transmit signal is restricted to lie in the set of only four alphabets, i.e.,

$$x_{t,n} \in \{\eta(\pm 1 \pm j)\},\ \forall\, t \in [T],\ \forall\, n \in [N],$$

where $\eta = \sqrt{P/2NT}$ with P being the total transmit power at each time slot and j is the imaginary unit. Throughout the paper, for a positive integer L, we denote $[L] = \{1, 2, \ldots, L\}$. For the communication users, the received signal matrix $\mathbf{Y} = [\mathbf{y}_1, \mathbf{y}_2, \ldots, \mathbf{y}_T] \in \mathbb{C}^{K\times T}$ is given by

$$\mathbf{Y} = \mathbf{H}\mathbf{X} + \mathbf{N},$$

where $\mathbf{H} = [\mathbf{h}_1, \mathbf{h}_2, \ldots, \mathbf{h}_K]^{\mathsf{T}} \in \mathbb{C}^{K\times N}$ is the channel matrix between the transmitter and the users, and $\mathbf{N} = [\mathbf{n}_1, \mathbf{n}_2, \ldots, \mathbf{n}_T] \in \mathbb{C}^{K\times T}$ is the additive white Gaussian noise matrix.

B. Performance Metric

In this part, we introduce the communication and radar metrics adopted in the paper.

1) Communication Metric: Let $\mathbf{S} = [\mathbf{s}_1, \mathbf{s}_2, \ldots, \mathbf{s}_T] \in \mathbb{C}^{K\times T}$ be the data symbols for the users. In this paper, we focus on the M-ary phase-shift keying (PSK) constellation and adopt the CI metric proposed in [9] as the communication metric. The idea of CI is to shape the interference so that it aligns constructively with the signal of interest and pushes the signal farther away from the decision boundary, thereby maximizing the useful signal power and minimizing the symbol error probability (SEP) [22].

For illustration, we depict a piece of the decision region of 8-PSK constellation in Fig. 1, where $s_{t,k}$ and $y'_{t,k} := \mathbf{h}_k^{\mathsf{T}}\mathbf{x}_t$ denote the data symbol and the noise-free received signal of user k at time-slot t, respectively. The CI effect is measured by the distance from $y'_{t,k}$ to its closest decision boundary of $s_{t,k}$, i.e., $\min\{d_{t,k}^{(1)}, d_{t,k}^{(2)}\}$, a crucial quantity known as the safety margin [22]. It was shown in [23], [24] that the SEP can be both upper and lower bounded by an increasing function of $\min\{d_{t,k}^{(1)}, d_{t,k}^{(2)}\}$. Hence, the communication QoS requirement can be formulated as

$$\min\{d_{t,k}^{(1)}, d_{t,k}^{(2)}\} \geq b_{t,k},\ \forall\, t \in [T],\ \forall\, k \in [K], \tag{1}$$

where $b_{t,k} > 0$ is the lower bound of the safety margin determined solely by the SEP threshold.

Next we derive the explicit formula of $\min\{d_{t,k}^{(1)}, d_{t,k}^{(2)}\}$. First, by decomposing $y'_{t,k}$ along the decision boundaries as

$$y'_{t,k} = \alpha_{t,k}^A s_{t,k}^A + \alpha_{t,k}^B s_{t,k}^B, \tag{2}$$

where $s_{t,k}^A = s_{k,t} e^{-j\frac{\pi}{M}}$ and $s_{t,k}^B = s_{t,k} e^{j\frac{\pi}{M}}$ are the unit vectors on the decision boundaries, we have

$$\min\{d_{t,k}^{(1)}, d_{t,k}^{(2)}\} = \min\{\alpha_{t,k}^A, \alpha_{t,k}^B\} \sin\Omega;$$

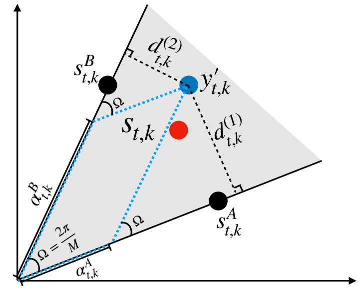

Fig. 1: An illustration of the CI metric.

see Fig. 1. By further rewriting (2) into the real space and noting that $y'_{t,k} = \mathbf{h}_k^{\mathsf{T}}\mathbf{x}_t$, we can express $\alpha_{t,k}^A$ and $\alpha_{t,k}^B$ as

$$\begin{pmatrix}\alpha_{t,k}^A\\ \alpha_{t,k}^B\end{pmatrix} = \frac{1}{\sin\Omega}\begin{pmatrix}\mathcal{I}(s_{t,k}^A) & -\mathcal{R}(s_{t,k}^A)\\ -\mathcal{I}(s_{t,k}^A) & \mathcal{R}(s_{t,k}^A)\end{pmatrix}\begin{pmatrix}\mathcal{R}(\mathbf{h}_k^{\mathsf{T}}) & -\mathcal{I}(\mathbf{h}_k^{\mathsf{T}})\\ \mathcal{I}(\mathbf{h}_k^{\mathsf{T}}) & \mathcal{R}(\mathbf{h}_k^{\mathsf{T}})\end{pmatrix}\begin{pmatrix}\mathcal{R}(\mathbf{x}_t)\\ \mathcal{I}(\mathbf{x}_t)\end{pmatrix}$$
$$=: \frac{1}{\sin\Omega}\begin{pmatrix}\mathbf{c}_{t,2k-1}^{\mathsf{T}}\\ \mathbf{c}_{t,2k}^{\mathsf{T}}\end{pmatrix}\begin{pmatrix}\mathcal{R}(\mathbf{x}_t)\\ \mathcal{I}(\mathbf{x}_t)\end{pmatrix}.$$

Let $\mathbf{x}_t^{\mathcal{R}} = [\mathcal{R}(\mathbf{x}_t)^{\mathsf{T}}\ \ \mathcal{I}(\mathbf{x}_t)^{\mathsf{T}}]^{\mathsf{T}} \in \mathbb{R}^{2N}$ be the real space representation of $\mathbf{x}_t$, $\mathbf{C}_t = [\mathbf{c}_{t,1}, \mathbf{c}_{t,2}, \ldots, \mathbf{c}_{t,2K-1}, \mathbf{c}_{t,2K}]^{\mathsf{T}} \in \mathbb{R}^{2K\times 2N}$, and $\mathbf{b}_t = [b_{t,1}, b_{t,2}, \ldots, b_{t,K}]^{\mathsf{T}} \otimes [1, 1]^{\mathsf{T}} \in \mathbb{R}^{2K}$, where $\otimes$ denotes the Kronecker product. Then the QoS constraint in (1) can be expressed as

$$\mathbf{C}_t\mathbf{x}_t^{\mathcal{R}} \geq \mathbf{b}_t,\ \forall\, t \in [T].$$

2) Radar Metric: A common radar metric is to match the transmit beampattern with a desired beampattern that is predetermined to ensure good sensing performance [25]. Note that for the considered model, the transmit beampattern at angle $\theta \in [-\pi/2, \pi/2]$ is given by $\mathbf{a}(\theta)^{\mathsf{H}}\mathbf{X}\mathbf{X}^{\mathsf{H}}\mathbf{a}(\theta)/T$, where $\mathbf{a}(\theta) := [1, e^{\pi\sin\theta}, \ldots, e^{j\pi(N-1)\sin\theta}]^{\mathsf{T}}$ is the steering vector. Let $d(\theta)$ be the desired beampattern. Then the radar metric is the difference between the designed and desired beampatterns:

$$\frac{1}{Q}\sum_{q=1}^{Q}\left|\alpha d(\theta_q) - \frac{1}{T}\mathbf{a}(\theta_q)^{\mathsf{H}}\mathbf{X}\mathbf{X}^{\mathsf{H}}\mathbf{a}(\theta_q)\right|^2,$$

where α is a scaling factor and $\{\theta_q\}_{q=1}^{Q}$ are the sampled angles.

C. Problem Formulation

Based on the above discussions, the one-bit transmit signal design problem, aiming to minimize the difference between the transmit and desired beampattern while satisfying the CI-based QoS requirement, can be formulated as follows:

$$\min_{\alpha>0,\mathbf{X}}\ \frac{1}{Q}\sum_{q=1}^{Q}\left|\alpha d(\theta_q) - \frac{1}{T}\mathbf{a}(\theta_q)^{\mathsf{H}}\mathbf{X}\mathbf{X}^{\mathsf{H}}\mathbf{a}(\theta_q)\right|^2, \tag{3a}$$
$$\text{s.t.}\quad \mathbf{C}_t\mathbf{x}_t^{\mathcal{R}} \geq \mathbf{b}_t,\ \forall\, t \in [T], \tag{3b}$$
$$x_{t,n} \in \{\eta(\pm 1 \pm j)\},\ \forall\, t \in [T],\ \forall\, n \in [N], \tag{3c}$$

where we recall that $\mathbf{X} = [\mathbf{x}_1, \mathbf{x}_2, \ldots, \mathbf{x}_T]$ and $\mathbf{x}_t^{\mathcal{R}}$ is the real-space counterpart of $\mathbf{x}_t$. To solve (3), we first note that for a given $\mathbf{X}$, the problem is quadratic in α, which admits a closed-form solution as

$$\alpha^*(\mathbf{X}) = \frac{\frac{1}{T}\sum_{q=1}^{Q} d(\theta_q)\mathbf{a}(\theta_q)^{\mathsf{H}}\mathbf{X}\mathbf{X}^{\mathsf{H}}\mathbf{a}(\theta_q)}{\sum_{q=1}^{Q} d^2(\theta_q)}.$$

By substituting $\alpha^*(\mathbf{X})$ into the objective function (3a) and transforming both the objective function (3a) and the one-bit constraint (3c) into the real space, we obtain the following equivalent real-space formulation (where a constant scaling factor has been omitted in the objective function):

$$\begin{aligned}\min_{\{\mathbf{x}_t^{\mathcal{R}}\}} \quad & \sum_{q=1}^{Q}\left(\sum_{t=1}^{T}\|\mathbf{A}_q\mathbf{x}_t^{\mathcal{R}}\|_2^2\right)^2-\left(\sum_{q=1}^{Q}\sum_{t=1}^{T}c_q\|\mathbf{A}_q\mathbf{x}_t^{\mathcal{R}}\|_2^2\right)^2 \\ \text{s.t.} \quad & \mathbf{C}_t\mathbf{x}_t^{\mathcal{R}}\geq\mathbf{b}_t,\ \forall\, t\in[T], \\ & x_{t,n}^{\mathcal{R}}\in\{-\eta,\eta\},\ \forall\, t\in[T],\ \forall\, n\in[2N],\end{aligned} \tag{4}$$

where

$$c_q=\frac{d(\theta_q)}{\sqrt{\sum_{q=1}^{Q}d^2(\theta_q)}},\ \mathbf{A}_q=\begin{pmatrix}\mathcal{R}(\mathbf{a}(\theta_q)) & \mathcal{I}(\mathbf{a}(\theta_q))\\ -\mathcal{I}(\mathbf{a}(\theta_q)) & \mathcal{R}(\mathbf{a}(\theta_q))\end{pmatrix}\in\mathbb{R}^{2\times 2N}.$$

III. Proposed Algorithm

Problem (4) is a large-scale discrete optimization problem with a nonconvex objective function and many linear constraints, which is challenging to solve. In this section, we propose an efficient algorithm for solving (4) by carefully exploiting its special structure.

A. Penalty Model

We first use the penalty technique [11], [26] to deal with the discrete one-bit constraint. Specifically, we relax the one-bit constraint to a boxed constraint and include a negative square penalty term into the objective function:

$$\begin{aligned}\min_{\{\mathbf{x}_t^{\mathcal{R}}\}} \quad & \sum_{q=1}^{Q}\left(\sum_{t=1}^{T}\|\mathbf{A}_q\mathbf{x}_t^{\mathcal{R}}\|_2^2\right)^2 \\ & -\left(\sum_{q=1}^{Q}\sum_{t=1}^{T}c_q\|\mathbf{A}_q\mathbf{x}_t^{\mathcal{R}}\|_2^2\right)^2-\lambda\sum_{t=1}^{T}\|\mathbf{x}_t^{\mathcal{R}}\|_2^2 \\ \text{s.t.} \quad & \mathbf{C}_t\mathbf{x}_t^{\mathcal{R}}\geq\mathbf{b}_t,\ \forall\, t\in[T], \\ & x_{t,n}^{\mathcal{R}}\in[-\eta,\eta],\ \forall\, t\in[T],\ \forall\, n\in[2N],\end{aligned} \tag{5}$$

where λ is the penalty parameter. The idea is that the negative square penalty would encourage large values for each element of $\mathbf{x}_t^{\mathcal{R}}$, so that a feasible discrete solution is likely to be attained when the penalty parameter λ is sufficiently large.

In our implementation, following a common technique in penalty-based approaches, we initialize the penalty parameter λ with a small value and gradually increase it, tracking the solution path of the corresponding penalty models. This simple technique has been shown to be able to significantly enhance the quality of the solution [12].

B. Inexact ALM Algorithm for Solving (5)

Next, we propose an inexact ALM framework for solving the penalty model (5).

1) Reformulation of (5)*:* We first introduce auxiliary variables $\mathbf{w}_{q,t}=\mathbf{A}_q\mathbf{x}_t^{\mathcal{R}}\in\mathbb{R}^2$ to simplify the objective function and introduce $\mathbf{z}_t\geq\mathbf{0}$ to transform the inequality linear constraints into equality ones:

$$\begin{aligned}\min \quad & \sum_{q=1}^{Q}\left(\sum_{t=1}^{T}\|\mathbf{w}_{q,t}\|_2^2\right)^2-\left(\sum_{q=1}^{Q}\sum_{t=1}^{T}c_q\|\mathbf{w}_{q,t}\|_2^2\right)^2-\lambda\sum_{t=1}^{T}\|\mathbf{x}_t^{\mathcal{R}}\|_2^2 \\ \text{s.t.} \quad & \mathbf{C}_t\mathbf{x}_t^{\mathcal{R}}-\mathbf{z}_t=\mathbf{b}_t,\ \mathbf{z}_t\geq\mathbf{0},\ \forall\, t\in[T], \\ & \tilde{\mathbf{A}}\mathbf{x}_t^{\mathcal{R}}-\mathbf{w}_t=\mathbf{0},\ \forall\, t\in[T], \\ & x_{t,n}^{\mathcal{R}}\in[-\eta,\eta],\ \forall\, t\in[T],\ \forall\, n\in[2N],\end{aligned}$$

where $\tilde{\mathbf{A}}=[\mathbf{A}_1^{\mathsf{T}},\mathbf{A}_2^{\mathsf{T}},\ldots,\mathbf{A}_Q^{\mathsf{T}}]^{\mathsf{T}}\in\mathbb{R}^{2Q\times 2N}$ and $\mathbf{w}_t=[\mathbf{w}_{1,t}^{\mathsf{T}},\mathbf{w}_{2,t}^{\mathsf{T}},\ldots,\mathbf{w}_{Q,t}^{\mathsf{T}}]^{\mathsf{T}}\in\mathbb{R}^{2Q\times 1}$. For conciseness, we further express the above problem into the following more compact form:

$$\begin{aligned}\min_{\mathbf{x}\in\mathcal{X},\mathbf{w},\mathbf{z}\in\mathcal{Z}} \quad & f(\mathbf{w})+g(\mathbf{w})+h(\mathbf{x}) \\ \text{s.t.} \quad & \mathbf{C}\mathbf{x}-\mathbf{z}=\mathbf{b}, \\ & \mathbf{A}\mathbf{x}-\mathbf{w}=\mathbf{0},\end{aligned} \tag{6}$$

where $\mathbf{x}=[(\mathbf{x}_1^{\mathcal{R}})^{\mathsf{T}},(\mathbf{x}_2^{\mathcal{R}})^{\mathsf{T}},\ldots,(\mathbf{x}_T^{\mathcal{R}})^{\mathsf{T}}]^{\mathsf{T}}$, $\mathbf{w}=[\mathbf{w}_1^{\mathsf{T}},\mathbf{w}_2^{\mathsf{T}},\ldots,\mathbf{w}_T^{\mathsf{T}}]^{\mathsf{T}}$, $\mathbf{z}=[\mathbf{z}_1^{\mathsf{T}},\mathbf{z}_2^{\mathsf{T}},\ldots,\mathbf{z}_T^{\mathsf{T}}]^{\mathsf{T}}$, $\mathbf{b}=[\mathbf{b}_1^{\mathsf{T}},\mathbf{b}_2^{\mathsf{T}},\ldots,\mathbf{b}_T^{\mathsf{T}}]^{\mathsf{T}}$, $\mathbf{C}=\operatorname{diag}(\mathbf{C}_1,\mathbf{C}_2,\ldots,\mathbf{C}_T)$, $\mathbf{A}=\mathbf{I}_T\otimes\tilde{\mathbf{A}}$, $\mathcal{X}=[-\eta,\eta]^{2NT}$, $\mathcal{Z}=\{\mathbf{z}\mid\mathbf{z}\geq\mathbf{0}\}$, and $f(\mathbf{w}),g(\mathbf{w})$, and $h(\mathbf{x})$ are the first, second, and third terms of the objective function, respectively.

2) Inexact ALM Framework: The ALM [27] is a popular and powerful method for solving (equality) constrained optimization problems like (6). Specifically, the augmented Lagrangian function of (6) is given by

$$\begin{aligned}\mathcal{L}_{\boldsymbol{\rho}}(\mathbf{x},\mathbf{w},\mathbf{z};\boldsymbol{\mu},\boldsymbol{\nu})=&f(\mathbf{w})+g(\mathbf{w})+h(\mathbf{x}) \\ &+\boldsymbol{\mu}^{\mathsf{T}}(\mathbf{C}\mathbf{x}-\mathbf{z}-\mathbf{b})+\boldsymbol{\nu}^{\mathsf{T}}(\mathbf{A}\mathbf{x}-\mathbf{w}) \\ &+\frac{\rho_\mu}{2}\|\mathbf{C}\mathbf{x}-\mathbf{z}-\mathbf{b}\|_2^2+\frac{\rho_\nu}{2}\|\mathbf{A}\mathbf{x}-\mathbf{w}\|_2^2,\end{aligned} \tag{7}$$

where $\boldsymbol{\mu}$ and $\boldsymbol{\nu}$ are the Lagrange multipliers and $\boldsymbol{\rho}:=(\rho_\mu,\rho_\nu)$ are the penalty parameters. For the classical ALM algorithm, we need to solve the following subproblem

$$(\mathbf{x}^m,\mathbf{w}^m,\mathbf{z}^m)\in\min_{\mathbf{x}\in\mathcal{X},\mathbf{w},\mathbf{z}\in\mathcal{Z}}\mathcal{L}_{\boldsymbol{\rho}^m}(\mathbf{x},\mathbf{w},\mathbf{z};\boldsymbol{\mu}^{m-1},\boldsymbol{\nu}^{m-1}) \tag{8}$$

at each iteration. To reduce the high computational cost of exactly solving (8), we propose an inexact ALM framework in Algorithm 1, which only requires an approximate stationary solution satisfying (9) at each iteration.

Algorithm 1 Inexact ALM framework for solving (6)

Input: $\boldsymbol{\mu}^0,\boldsymbol{\nu}^0,\tau>1,\delta>0$, a positive sequence $\epsilon_m\to 0$.
for $m=1,2,\ldots$ **do**
Step 1: *(Solve the ALM subproblem)*: Find $(\mathbf{x}^m,\mathbf{w}^m,\mathbf{z}^m)$ that satisfies

$$\begin{aligned}\operatorname{dist}\big(&\nabla\mathcal{L}_{\boldsymbol{\rho}^m}(\mathbf{x}^m,\mathbf{w}^m,\mathbf{z}^m;\boldsymbol{\mu}^{m-1},\boldsymbol{\nu}^{m-1}) \\ &+\partial\mathbb{I}_{\mathcal{X}}(\mathbf{x}^m)+\partial\mathbb{I}_{\mathcal{Z}}(\mathbf{z}^m),\mathbf{0}\big)\leq\epsilon_m.\end{aligned} \tag{9}$$

Step 2: *(Update the Lagrange multipliers)*

$$\boldsymbol{\mu}^m=\boldsymbol{\mu}^{m-1}+\rho_\mu^m(\mathbf{C}\mathbf{x}^m-\mathbf{z}^m-\mathbf{b}),$$
$$\boldsymbol{\nu}^m=\boldsymbol{\nu}^{m-1}+\rho_\nu^m(\mathbf{A}\mathbf{x}^m-\mathbf{w}^m).$$

Step 3: *(Update the penalty parameter)*

$$\rho_\mu^{m+1}=\tau\rho_\mu^m,\ \rho_\nu^{m+1}=\tau\rho_\nu^m.$$

end for

To obtain a solution satisfying (9) at each iteration, we next propose a custom-designed BSUM algorithm for approximately solving the ALM subproblem.

3) BSUM Algorithm for Solving Subproblem (8)*:* Noting that the constraints in the ALM subproblem (8) are separable within each block of variables $\{\mathbf{x},\mathbf{w},\mathbf{z}\}$, it is convenient to update the variables alternately to solve the problem. By carefully exploiting the problem structure, we propose the following algorithm:

$$\mathbf{x}^{(r+1)} \in \arg\min_{\mathbf{x}\in\mathcal{X}} \nabla \mathcal{L}_{\boldsymbol{\rho}^m}(\mathbf{x}^{(r)}, \mathbf{w}^{(r)}, \mathbf{z}^{(r)}; \boldsymbol{\mu}^{m-1}, \boldsymbol{\nu}^{m-1})^{\mathsf{T}}(\mathbf{x} - \mathbf{x}^{(r)}) + \frac{\gamma^m}{2}\|\mathbf{x} - \mathbf{x}^{(r)}\|_2^2, \tag{10a}$$

$$\mathbf{w}^{(r+1)} \in \arg\min f(\mathbf{w}) + \nabla g(\mathbf{w}^{(r)})^{\mathsf{T}}(\mathbf{w} - \mathbf{w}^{(r)}) - (\boldsymbol{\nu}^{m-1})^{\mathsf{T}}\mathbf{w} + \frac{\rho_v^m}{2}\|\mathbf{w} - \mathbf{A}\mathbf{x}^{(r+1)}\|_2^2, \tag{10b}$$

$$\mathbf{z}^{(r+1)} \in \arg\min_{\mathbf{z}\in\mathcal{Z}} -(\boldsymbol{\mu}^{m-1})^{\mathsf{T}}\mathbf{z} + \frac{\rho_\mu^m}{2}\|\mathbf{z} - \mathbf{C}\mathbf{x}^{(r+1)} + \mathbf{b}\|_2^2. \tag{10c}$$

The above algorithm falls into the category of the BSUM algorithm [28] as the $\mathbf{x}$-, $\mathbf{w}$-, and $\mathbf{z}$-subproblems, with some constant terms added, minimize an upper bound of the current objective function of (8) at each iteration, as long as $\gamma^m \geq \|\rho_\mu^m \mathbf{C}^{\mathsf{T}}\mathbf{C} + \rho_v^m \mathbf{A}^{\mathsf{T}}\mathbf{A}\|_2$. This can be easily verified by the concavity of $g(\mathbf{w})$ and $h(\mathbf{x})$. Hence, by the property of BSUM [28], an approximate stationary solution satisfying (9) can be obtained within a finite number of iterations.

Moreover, problems (10a)–(10c) all admit closed-form solutions, making the proposed BSUM algorithm computationally efficient. First, it is obvious that the $\mathbf{x}$- and $\mathbf{z}$-subproblems only involve projections onto the sets $\mathcal{X} = [-\eta, \eta]^{2NT}$ and $\mathcal{Z} = \{\mathbf{z} \mid \mathbf{z} \geq \mathbf{0}\}$, respectively, which admit closed-form solutions. For the $\mathbf{w}$-subproblem, by linearizing $g(\mathbf{w})$, the problem becomes separable over the index $q \in [Q]$. Let $\mathbf{w}_{(q)} := [\mathbf{w}_{q,1}^{\mathsf{T}}, \mathbf{w}_{q,2}^{\mathsf{T}}, \ldots, \mathbf{w}_{q,T}^{\mathsf{T}}]^{\mathsf{T}}$ denote the vector collecting all the components in $\mathbf{w}$ related to q and let $\boldsymbol{\xi}_q^{(r)}$ be the coefficient of the linear term in (10b) related to $\mathbf{w}_{(q)}$. Then for each $q \in [Q]$, the $\mathbf{w}_{(q)}$-subproblem has the following form:

$$\mathbf{w}_{(q)}^{(r+1)} = \arg\min_{\mathbf{w}_{(q)}} \|\mathbf{w}_{(q)}\|_2^4 + \frac{\rho_v^m}{2}\|\mathbf{w}_{(q)}\|_2^2 + (\boldsymbol{\xi}_q^{(r)})^{\mathsf{T}}\mathbf{w}_{(q)}.$$

Clearly, the optimal direction of $\mathbf{w}_{(q)}$ is given by $-\boldsymbol{\xi}_q^{(r)}/\|\boldsymbol{\xi}_q^{(r)}\|$. Therefore, we only need to optimize the norm of $\mathbf{w}_{(q)}$, i.e., solving a univariate quartic problem as follows:

$$\beta_q^{(r)} \in \arg\min_{\beta\geq 0} \left\{\beta^4 + \frac{\rho_v^m}{2}\beta^2 - \left\|\boldsymbol{\xi}_q^{(r)}\right\|\beta\right\},$$

whose explicit solution can be obtained by solving a cubic equation. Then, we get

$$\mathbf{w}_{(q)}^{(r+1)} = -\frac{\beta_q^{(r)}}{\|\boldsymbol{\xi}_q^{(r)}\|}\boldsymbol{\xi}_q^{(r)}, \ \forall\, q \in [Q].$$

IV. Simulation Results

In this section, we present simulation results to evaluate the performance of the proposed algorithm. As in [1], the elements of the channel $\mathbf{H}$ are i.i.d. generated following $\mathcal{CN}(0, 1)$ and the transmit power is set as $P = 1$. The block length is $T = 50$. We focus on QPSK constellation and consider the following desired beampattern:

$$d(\theta) = \begin{cases} 1, & \text{if } \theta \in \left[\theta_i - \dfrac{\Delta_\theta}{2}, \theta_i + \dfrac{\Delta_\theta}{2}\right], \ i = 1, 2, 3; \\ 0, & \text{otherwise}, \end{cases}$$

where $\theta_1 = -40°$, $\theta_2 = 0°$, and $\theta_3 = 40°$ are the angles of interest to be explored, and $\Delta_\theta = 10°$ is the beam width. The direction grids $\{\theta_q\}$ are uniformly sampled from $-90°$ to $90°$ with a resolution of $1°$. For comparison, we include the algorithms in [1] and the MVAM algorithm in [17] as benchmarks. Note that the algorithm in [1] is designed for the infinite-resolution case, which we term as "Inf-Res" in the simulation. We also include a quantized version of the algorithm in [1] by directly quantizing its output to satisfy the one-bit constraint, which is termed as "Quantize".

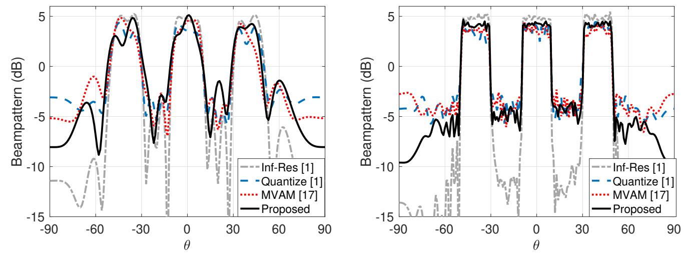

(a) $N = 16,\ K = 2$. (b) $N = 64,\ K = 4$.

Fig. 2: Beampattern for different algorithms.

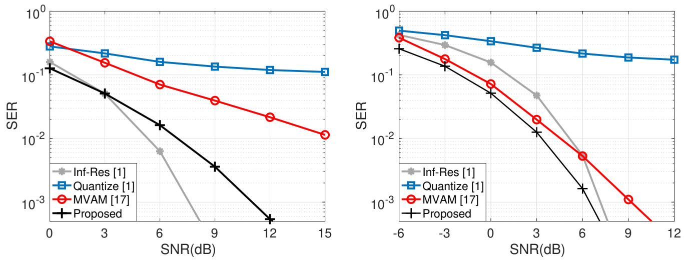

(a) $N = 16,\ K = 2$. (b) $N = 64,\ K = 4$.

Fig. 3: SER performance for different algorithms.

In Fig. 2, we depict the beampattern of the compared approaches. As can be observed from the figure, there is a degradation in radar performance when one-bit DACs are employed. Nevertheless, the three one-bit approaches still produce satisfactory beampatterns, featuring strong mainlobes around the desired angles. Notably, the proposed approach demonstrates the best beampattern among them.

In Fig. 3, we evaluate the SER performance of the compared approaches. All the results are averaged over 500 channel realizations. As shown in the figure, there is a severe error rate floor if we directly quantize the output of the algorithm in [1]. In contrast, the MVAM algorithm in [17] and the proposed algorithm, which are designed specifically for the one-bit scenario, achieve significantly better SER performance. Due to the superiority of their problem formulations, these two one-bit approaches even outperform the unquantized version of the algorithm in [1] (corresponding to the case where infinite-resolution DACs are employed) in large systems and at low SNRs; see Fig. 3 (b). Finally, we note that for the two one-bit approaches, the proposed one performs much better, especially in high SNR cases.

From the simulations, we can conclude that the proposed approach achieves substantially better radar and communication performance compared to the existing approaches. This is attributed to both the superiority of the CI metric compared to the MSE metric and the effectiveness of the proposed algorithm.

REFERENCES

[1] F. Liu, L. Zhou, C. Masouros, A. Li, W. Luo, and A. Petropulu, "Toward dual-functional radar-communication systems: Optimal waveform design," *IEEE Trans. Signal Process.*, vol. 66, no. 16, pp. 4264–4279, Aug. 2018.

[2] X. Liu, T. Huang, N. Shlezinger, Y. Liu, J. Zhou, and Y. C. Eldar, "Joint transmit beamforming for multiuser MIMO communications and MIMO radar," *IEEE Trans. Signal Process.*, vol. 68, pp. 3929–3944, 2020.

[3] F. Liu, Y.-F. Liu, A. Li, C. Masouros, and Y. C. Eldar, "Cramér-Rao bound optimization for joint radar-communication beamforming," *IEEE Trans. Signal Process.*, vol. 70, pp. 240–253, 2022.

[4] Z. Wang, J. Wu, Y.-F. Liu, and F. Liu, "Globally optimal beamforming design for integrated sensing and communication systems," 2023. [Online]. Available: http://arxiv.org/abs/2309.06674

[5] F. Rusek, D. Persson, B. K. Lau, E. G. Larsson, T. L. Marzetta, O. Edfors, and F. Tufvesson, "Scaling up MIMO: Opportunities and challenges with very large arrays," *IEEE Signal Process. Mag.*, vol. 30, no. 1, pp. 40–60, Jan. 2013.

[6] B. Razavi, *Principles of Data Conversion System Design*, 1st ed. Hoboken, NJ, USA: Wiley, 1994.

[7] S. Jacobsson, G. Durisi, M. Coldrey, T. Goldstein, and C. Studer, "Quantized precoding for massive MU-MIMO," *IEEE Trans. Commun.*, vol. 65, no. 11, pp. 4670–4684, Nov. 2017.

[8] H. Jedda, A. Mezghani, J. A. Nossek, and A. L. Swindlehurst, "Massive MIMO downlink 1-bit precoding with linear programming for PSK signaling," in *Proc. IEEE Workshop Signal Process. Adv. Wireless Commun.*, Jul. 2017, pp. 1–5.

[9] A. Li, C. Masouros, F. Liu, and A. L. Swindlehurst, "Massive MIMO 1-bit DAC transmission: A low-complexity symbol scaling approach," *IEEE Trans. Wireless Commun.*, vol. 17, no. 11, pp. 7559–7575, Nov. 2018.

[10] F. Sohrabi, Y.-F. Liu, and W. Yu, "One-bit precoding and constellation range design for massive MIMO with QAM signaling," *IEEE J. Sel. Topics Signal Process.*, vol. 12, no. 3, pp. 557–570, Jun. 2018.

[11] M. Shao, Q. Li, W.-K. Ma, and A. M.-C. So, "A framework for one-bit and constant-envelope precoding over multiuser massive MISO channels," *IEEE Trans. Signal Process.*, vol. 67, no. 20, pp. 5309–5324, Oct. 2019.

[12] Z. Wu, B. Jiang, Y.-F. Liu, M. Shao, and Y.-H. Dai, "Efficient CI-based one-bit precoding for multiuser downlink massive MIMO systems with PSK modulation," *IEEE Trans. Wireless Commun. (early access)*, 2023.

[13] A. K. Saxena, I. Fijalkow, and A. L. Swindlehurst, "Analysis of one-bit quantized precoding for the multiuser massive MIMO downlink," *IEEE Trans. Signal Process.*, vol. 65, no. 17, pp. 4624–4634, Sept. 2017.

[14] Z. Wu, J. Ma, Y.-F. Liu, and A. Lee Swindlehurst, "Asymptotic SEP analysis and optimization of linear-quantized precoding in massive MIMO systems," *IEEE Trans. Inf. Theory (early access)*, 2023.

[15] A. Li, C. Masouros, A. L. Swindlehurst, and W. Yu, "1-bit massive MIMO transmission: Embracing interference with symbol-level precoding," *IEEE Commun. Mag.*, vol. 59, no. 5, pp. 121–127, May 2021.

[16] Z. Cheng, S. Shi, Z. He, and B. Liao, "Transmit sequence design for dual-function radar-communication system with one-bit DACs," *IEEE Trans. Wireless Commun.*, vol. 20, no. 9, pp. 5846–5860, Sept. 2021.

[17] X. Yu, Q. Yang, Z. Xiao, H. Chen, V. Havyarimana, and Z. Han, "A precoding approach for dual-functional radar-communication system with one-bit DACs," *IEEE J. Sel. Areas Commun.*, vol. 40, no. 6, pp. 1965–1977, Jun. 2022.

[18] J. Yan and J. Zheng, "Transmit signal design of MIMO dual-function radar communication with 1-bit DACs," in *Proc. IEEE Workshop Signal Process. Adv. Wireless Commun.*, Jul. 2022, pp. 1–5.

[19] R. Liu, M. Li, Q. Liu, and A. L. Swindlehurst, "Dual-functional radar-communication waveform design: A symbol-level precoding approach," *IEEE J. Sel. Topics Signal Process.*, vol. 15, no. 6, pp. 1316–1331, Nov. 2021.

[20] Z. Zhang, Q. Chang, F. Liu, and S. Yang, "Dual-functional radar-communication waveform design: Interference reduction versus exploitation," *IEEE Commun. Lett.*, vol. 26, no. 1, pp. 148–152, Jan. 2022.

[21] N. Su, F. Liu, Z. Wei, Y.-F. Liu, and C. Masouros, "Secure dual-functional radar-communication transmission: Exploiting interference for resilience against target eavesdropping," *IEEE Trans. Wireless Commun.*, vol. 21, no. 9, pp. 7238–7252, Sept. 2022.

[22] C. Masouros and G. Zheng, "Exploiting known interference as green signal power for downlink beamforming optimization," *IEEE Trans. Signal Process.*, vol. 63, no. 14, pp. 3628–3640, Jul. 2015.

[23] M. Shao, Q. Li, Y. Liu, and W.-K. Ma, "Multiuser one-bit massive MIMO precoding under MPSK signaling," in *Proc. IEEE Global Conf. Signal Inf. Process.*, Nov. 2018, pp. 833–837.

[24] Z. Wu, J. Wu, W.-K. Chen, and Y.-F. Liu, "Diversity order analysis for quantized constant envelope transmission," *IEEE Open J. Signal Process.*, vol. 4, pp. 21–30, 2023.

[25] P. Stoica, J. Li, and Y. Xie, "On probing signal design for MIMO radar," *IEEE Trans. on Signal Process.*, vol. 55, no. 8, pp. 4151–4161, Aug. 2007.

[26] Y.-F. Liu, T.-H. Chang, M. Hong, Z. Wu, A. M.-C. So, E. A. Jorswieck, and W. Yu, "A survey of advances in optimization methods for wireless communication system design," 2024. [Online]. Available: http://arxiv.org/abs/2401.12025

[27] J. Nocedal and S. J. Wright, *Numerical Optimization*, 2nd ed. New York, NY, USA: Springer, 2006.

[28] M. Razaviyayn, M. Hong, and Z.-Q. Luo, "A unified convergence analysis of block successive minimization methods for nonsmooth optimization," *SIAM J. Optim.*, vol. 23, no. 2, pp. 1126–1153, 2013.